10.1109/ULTSYM.2014.0152

Quantitative ultrasound analyses of cell starvation in HT-29 pellets

L.A. Wirtzfeld[1], E.S.L. Berndl[1], G.J. Czarnota[2] and M.C. Kolios[1]

[1]Department of Physics, Faculty of Science
Ryerson University
Toronto, Ontario, Canada
mkolios@ryerson.ca

[2]Department of Radiation Oncology and Imaging
Sunnybrook Health Sciences Centre
Toronto, Ontario, Canada

***Abstract*—Spectral analysis of ultrasound backscatter data has been shown to be sensitive to cellular changes, particularly due to apoptosis. Different therapies that seek to destroy cells work activate different cell death mechanisms, most commonly apoptosis, but also oncosis or ischemic death. Pellets of HT-29 colon adenocarcinoma cells were placed in PBS at room temperature over the course of 56 hours and were imaged with high-frequency (55 MHz) ultrasound and the raw RF data processed. Due to the lack of nutrients available to the cells, they underwent oncosis. Attenuation slope, speed of sound (SOS), spectral slope and midband fit (MBF) were estimated every 8 hours over the course of 56 hours to determine changes due to starvation. The spectral slope decreased through time, with an increase at 40 hours. Midband fit and attenuation both showed a trend through time with three phases with the first significant increase at 16 hours and a second significant increase at 40 hours. Speed of sound increased from 1513 m/s to 1534 m/s with time. A decrease in cellular number density and increase in inter-cellular debris is evident on histological slides. Results show different trends than observed for cells undergoing apoptosis, suggesting there are specific signatures that can be exploited to determine changes in cell morphology associated with different mechanisms of cell death.**

Keywords— High-frequency ultrasound, HT-29 cell pellet, oncosis, quantitative ultrasound, spectral analysis

I. INTRODUCTION

The ability to non-invasively monitor and detect changes in tissue microstructure through time has the potential to impact how we assess clinical treatments, especially in oncology. Different types of cell death should have different signatures in spectral and quantitative ultrasound techniques as the change in cellular architecture is unique to each method of cell death. Apoptosis is frequently studied as the result of chemotherapeutics and radiation treatment on cancer cells. Apoptosis, or programmed cell death, involves the shrinking of cell volume due to blebbing. Less well studied is oncosis, in which a cell swells [1]. Both apoptosis and oncosis lead to necrosis, which is the degradation of cells following cell death [2-3]. Apoptosis has been studied extensively due to its role in chemotherapy and cancer. [2-5]

Necrosis has shown ultrasound contrast in spheroids [6] and in tumor cores, however, changes in spectral parameters have not been evaluated. Apoptosis has been studied in more detail, with changes in ultrasound spectral parameters observed as cells undergo apoptosis due to chemotherapeutic treatments, in cell pellets and individual cells [7].

A comparison of apoptotic versus oncotic cell death was performed using AML cells at room temperature for 5 hours [1]. The oncotic cells were not monitored beyond this time point and out to the lengths where changes in apoptosis continue to be evident (i.e. after 24 and 48 hours). The complimentary techniques to those developed for ultrasound spectral analysis have been used for the comparison of pellets with cells undergoing apoptosis, mitotic arrest and necrosis using optical coherence tomography quantitative techniques and have shown differing trends between necrosis and apoptosis for parameters such as the spectral slope [8].

This study tracks pellets of colon adenocarcinoma cells in PBS at room temperature over a course of 56 hours. The pellets allow for analysis of an ensemble of identical cells, without contributions from extracellular components. Without nutrients from the media the cells are starved and will undergo oncosis and necrosis. Changes in attenuation slope, speed of sound, spectral slope and midband fit are monitored as the cells decay. Histological analysis of changes in cell size, viability and spacing is correlated with ultrasound changes.

II. MATERIALS AND METHODS

A. Pellet Model

HT-29 cells (ATCC) were grown in McCoy's 5A media prepared from powder (Gibco) at Princess Margaret Hospital (Toronto, ON), and supplemented with 10% FBS (Gibco). Cells were incubated at 37°C, 5% CO_2 in a humidified chamber and passed every 3 to 4 days to maintain the cells in the exponential growth phase until required for pellet preparation.

Ten cell pellets were prepared: two in a custom stainless steel holder with three wells with depth 3.02 mm and diameter of 7.8 mm for ultrasound imaging, and eight in 8 mm diameter flat bottomed tubes for histology. For each pellet, HT-29 cells were dissociated with trypsin and 30 million cells were placed in the well, and centrifuged for 10 minutes at 200x*g*. Excess media was gently removed, and the pellets were carefully

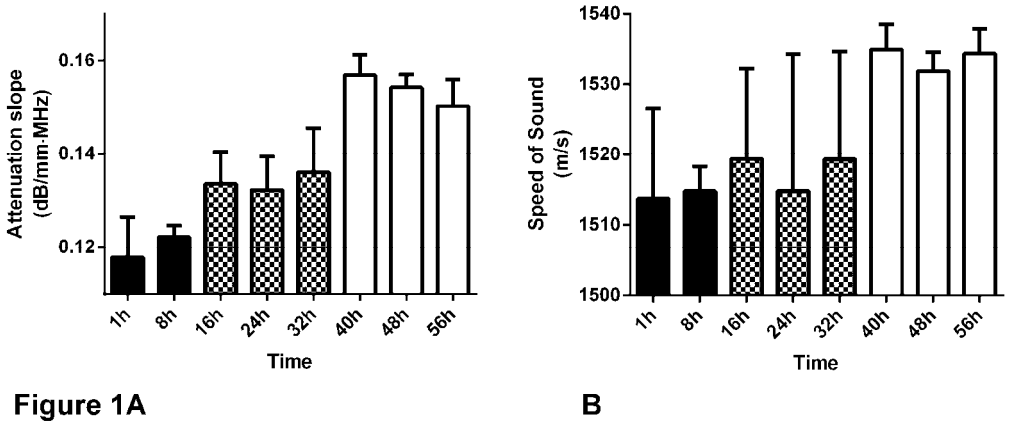

Figure 1A **B**

Fig. 1. Measurements of a) attenuation and b) speed of sound of pellets through time. Error bars represent standard deviations of all planes from the two cell pellets. Time points are grouped into early (black), middle (grey) or late (white) stages of starvation. Late stage SOS measurements are significantly different ($p<0.05$) from both early and middle stage measurements. Attenuation measurements at each time point have statistically significant differences ($p<0.05$) from times in other stages. Error bars represent ± SEM.

covered with phosphate buffered saline (PBS) and left at room temperature for the remainder of the experiment.

B. Data acquisition

Ultrasound data were acquired using a Vevo770 preclinical imaging system (VisualSonics, Toronto, ON) using a nominal 55 MHz single-element mechanically-scanned transducer. Raw radio frequency (RF) data was acquired and digitized on board at 420 MHz. Twelve planes of 100 A-lines were acquired from each of the two imaging pellets at each time point.

Reference data were acquired from the stainless steel at the bottom of the third well, which contained only PBS in order to normalize the data.

C. Histology and Staining

At each ultrasound time point, the PBS from one of the pellets in tubes for histology was carefully removed and replaced with neutral buffered formalin (NBF). All samples were left in NBF for at least 48 hours. Samples were removed from the tubes by cutting off the flat bottom, and were embedded in paraffin for histology.

Hematoxylin and Eosin (H&E) staining was completed using a Leica Autostainer XL (Leica Biosystems, Richmond, USA), and imaged using a Retiga 2000R Fast 1394 Color (QImaging) mounted on a CKX41 Olympus microscope, and captured using QCapture v2.90.1 (QImaging)

D. Ultrasound Data Processing

The total region of the pellet in the image was manually segmented to obtain the top and bottom of the pellet. For spectral analyses, the pellet was divided into 15 λ by 15 λ regions of interest (ROI) with 50% overlap both axially and laterally. All spectral analyses were performed for each ROI, which allows for local computation of parameters and parametric images to be displayed.

1) Attenuation: Attenuation was calculated using an insertion loss technique where the power spectrum from the planar reflector in the PBS only reference well was divided by the power spectrum from planar reflector beneath the pellet [9]. The attenuation was estimated for each scan line and divided by the pellet thickness at the same location. A linear fit was performed over the transducer bandwidth to estimate a linear attenuation coefficient which was averaged across scan lines to provide an estimate for each slice of data. Attenuation estimates for each pellet were used for attenuation compensation of the power spectra at each individual time point.

2) Speed of Sound: The background PBS was assumed to have a speed of sound (SOS) of 1500 m/s. The speed of sound in the pellet was calculated as

$$c_{pellet} = 2d/\Delta t \,, \tag{1}$$

where d is the thickness of the pellet calculated from the top of the pellet and the known location of the depth of the well from the PBS only reference well and Δt is the length of time between the echo arrival from the top of the pellet and the planar reflector beneath the pellet [1].

3) Power Spectra: Power spectra for each ROI were divided by the average power spectrum from the planar reflector to remove system effects. The spectra were also corrected for attenuation loss based on the, along the path from the top of the pellet to the center of the ROI, using the linear attenuation coefficient estimated at each time point.

Once the power spectra were corrected for the system effects and attenuation the linear regression was performed to calculate a spectral slope and midband fit (MBF) according to the methods developed by Lizzi et al. [10].

E. Statistical analysis

Two way ANOVAs were performed for each of the quantitative parameters to determine if there were changes in value between the pellets imaged. A p-value of less than 0.05 was considered significant and post-hoc comparisons

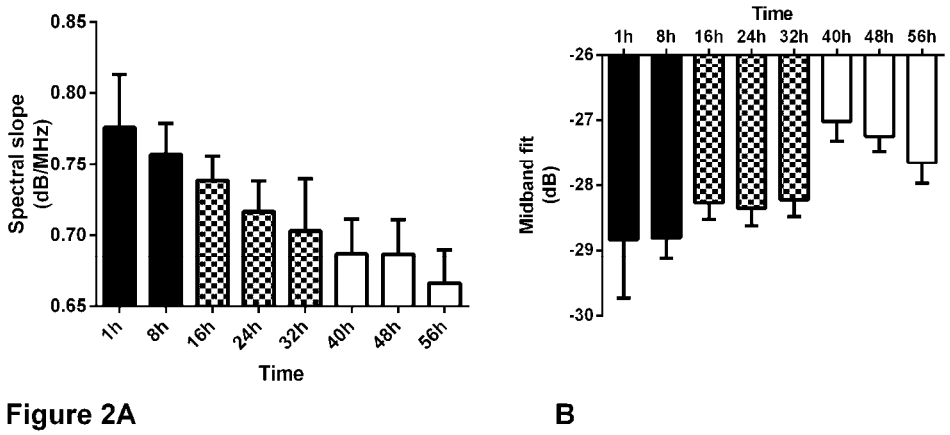

Fig. 2. Measurements of a) Spectral slope and b) midband fit of pellets through time. Error bars represent standard deviations of all planes from the two cell pellets. Time points are grouped into early (black), middle (grey) or late (white) stages of starvation. Measurements at each time point have sstatistically significant differences ($p<0.05$) from times in other stages. Error bars represent ± SEM.

by 95% confidence intervals were used to determine pairs that were significantly different.

III. Results

A. Attenuation

Attenuation slope (Fig. 1a) increased through time from 0.118 dB/mm MHz to a maximum of 0.157 dB/mm-MHz at 40 hours and decreased slightly beyond that time point. Three distinct phases were observed, the first from 1 to 8 hours, the second from 16 to 32 hours and lastly from 40 to 56 hours. In each of these phases, the attenuation was statistically significantly different from estimates in the other phases, but not estimates within the same phase. This result formed the basis of the separation of the phases.

B. Speed of Sound

The SOS (Fig.1b) show an overall gradual increase with time from 1513 m/s to 1534 m/s, with the time points from 40 hours on showing much lower standard deviation than earlier time points. There were statistically significant differences in SOS between the final phase and both of the earlier phases, but not between the early and middle stages.

C. Spectral slope

The attenuation compensated spectral slope (Fig. 2a) shows a gradual decrease through time from 0.78 dB/MHz at 1 hour to 0.67 dB/MHz at 56 hours with a plateau at 40 hours. There were statistically significant differences separated by any two time points, with the exception of the 40 to 48 hour time points which had the same slope and statistically significant differences were seen at time points 24 hours apart.

D. Midband Fit

The attenuation compensated MBF (Fig. 2b) increased from 1 hour through to 40 hours with a slight decrease beyond. The MBF results showed the same three phases observed for attenuation where estimates from 1 to 8 hour, 16 to 32 hours and 40 to 56 hours were statistically significantly different from time points in a different phase.

E. Histology correlation

Histological samples of pellets from time points 1 hour through to 48 hour were compared. The pellet at 56 hours fell apart during fixation, therefore histology cannot be compared at this time point. Fig. 3 shows example H&E slides at 1, 32, 40 and 48 hours showing an apparent decrease in cellular number density from 1 through 40 hours. An increase in extra-cellular debris is seen through time that is likely components of cellular membrane from cells that have died. The cell shape also gradually changes from round at 1 and 8 hours to more irregular shapes through time.

IV. Discussion

Our studies of attenuation, SOS, spectral slope and MBF indicate three distinct phases of decay due to starvation, indicated by changes in color in the figures. Generally, there are statistically significant differences between the stages, but not within them. These three stages appear to correspond to the initial stress of insufficient nutrients for cell maintenance, the cells being irrevocably set for cell death, and the actual process of the cells dying.

Previously, a study [11] showed fibroblasts growing in a monolayer without serum, a requirement for normal cell growth, which showed recoverable cell rounding after 10 hours, potentially corresponding to the first stage change observed in this paper. This was followed by unrecoverable cell rounding and dissociation from flasks at 24 hours, where these cells can no longer be rescued from the cell death pathways and which potentially corresponds to the second stage change between 24 and 32 hours. Finally, after 48 hours 50% of the cells are positive for TdT labeling, which is indicative of DNA damage and which could correspond to the third stage presented in this paper [11].

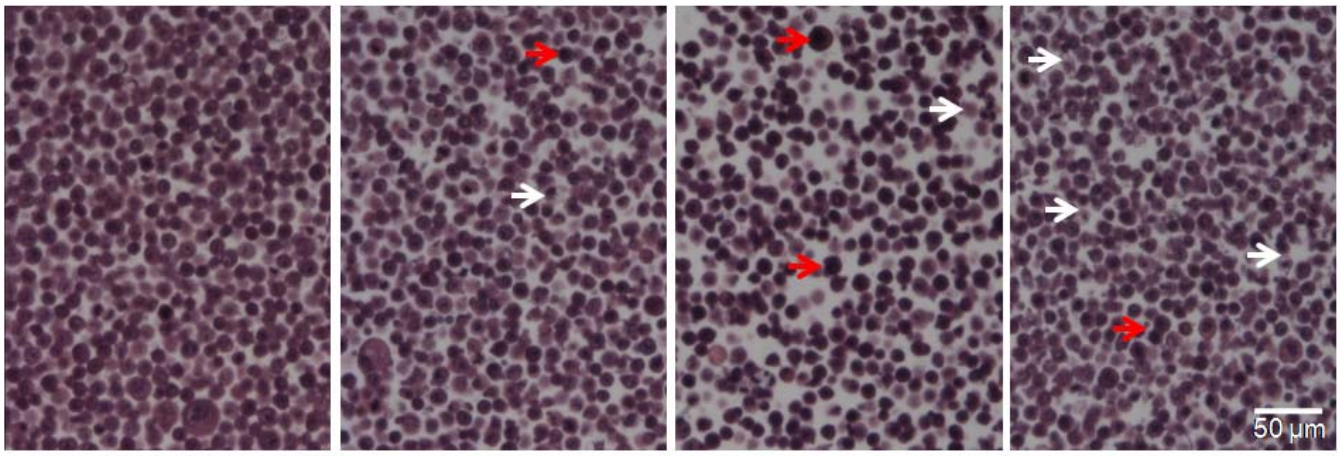

Fig. 3. Figure 3: H&E stained histology samples at time points of 1, 32, 40 and 48 hours. Structural changes in cell morphology are observed, such as increased nuclear staining (red arrows) and increased cellular fragmentation (white arrows) Moreover, an apparent decrease in cellular density in observed at 40 hours.

Comparative publications of cells undergoing apoptosis, particularly in a cell pellet, show the opposite trend in slope with the slope increasing through time as the cell undergoes apoptosis [7]. A consistent decrease is observed in this study as the cells in the pellets decay. A similar trend is observed compared to experiments with AML cell pellets undergoing oncotic cell , though the change in MBF over the entire course of 56 hours for the HT-29 carcinoma cells is less than observed over 5 hours for the AML pellets.

V. Conclusion:

Changes in cellular microstructure due to cell decay in conditions of starvation resulted in consistent and measurable changes in measurable, quantitative parameters from high-frequency ultrasound, including attenuation slope, SOS, spectral slope and MBF. The process is slow resulting in gradual changes until 40 hours where the trends either change or an inflection in the trend is observed. The ability to distinguish, using ultrasound, a variety of microstructural changes, including variations in the type of cell death, could provide additional clinical information on therapeutic responses in-vivo.

Acknowledgments

The authors would like to acknowledge funding from a project grant entitled “Imaging for Cancer” from the Terry Fox Foundation (CIHR#TFF 105267) and the Canadian Foundation for Innovation.

References

[1] M. C. Kolios, L. Taggart, R. E. Baddour, F. S. Foster, J. W. Hunt, G. J. Czarnota, and M. D. Sherar, “An investigation of backscatter power spectra from cells, cell pellets and microspheres,” in *2003 IEEE Symposium on Ultrasonics*, 2003, vol. 1, pp. 752–757 Vol.1.

[2] P. Weerasinghe and L. M. Buja, “Oncosis: An important non-apoptotic mode of cell death,” *Experimental and Molecular Pathology*, vol. 93, no. 3, pp. 302–308, Dec. 2012.

[3] G. Majno and I. Joris, “Apoptosis, oncosis, and necrosis. An overview of cell death.,” Am J Pathol, vol. 146, no. 1, pp. 3–15, Jan. 1995.

[4] S. Van Cruchten and W. Van den Broeck, “Morphological and Biochemical Aspects of Apoptosis, Oncosis and Necrosis,” *Anatomia, Histologia, Embryologia*, vol. 31, no. 4, pp. 214–223, Aug. 2002.

[5] H. Jaeschke and J. J. Lemasters, “Apoptosis versus oncotic necrosis in hepatic ischemia/reperfusion injury,” *Gastroenterology*, vol. 125, no. 4, pp. 1246–1257, Oct. 2003.

[6] M. D. Sherar, M. B. Noss, and F. S. Foster, “Ultrasound backscatter microscopy images the internal structure of living tumour spheroids,” *Nature*, vol. 330, no. 6147, pp. 493–495, Dec. 1987.

[7] M. C. Kolios, G. J. Czarnota, M. Lee, J. W. Hunt, and M. D. Sherar, “Ultrasonic spectral parameter characterization of apoptosis,” *Ultrasound in Medicine & Biology*, vol. 28, no. 5, pp. 589–597, May 2002.

[8] G. Farhat, V. X. D. Yang, G. J. Czarnota, and M. C. Kolios, “Detecting cell death with optical coherence tomography and envelope statistics,” *J Biomed Opt*, vol. 16, no. 2, p. 026017, Feb. 2011.

[9] K. A. Wear, T. A. Stiles, G. R. Frank, E. L. Madsen, F. Cheng, E. J. Feleppa, C. S. Hall, B. S. Kim, P. Lee, W. D. O’Brien Jr, M. L. Oelze, B. I. Raju, K. K. Shung, T. A. Wilson, and J. R. Yuan, “Interlaboratory comparison of ultrasonic backscatter coefficient measurements from 2 to 9 MHz,” *J Ultrasound Med*, vol. 24, no. 9, pp. 1235–1250, Sep. 2005.

[10] F. L. Lizzi, M. Greenebaum, E. J. Feleppa, M. Elbaum, and D. J. Coleman, “Theoretical framework for spectrum analysis in ultrasonic tissue characterization,” *J. Acoust. Soc. Am.*, vol. 73, no. 4, pp. 1366–1373, Apr. 1983.

[11] N. M. Hasan, G. E. Adams, and M. C. Joiner, “Effect of serum starvation on expression and phosphorylation of PKC-α and p53 in V79 cells: Implications for cell death,” *Int. J. Cancer*, vol. 80, no. 3, pp. 400–405, Jan. 1999.